

Electronic Supplementary Information

Unraveling Na-ion storage performance of vertically-aligned interlayer-expanded two-dimensional MoS₂@C@MoS₂ heterostructure

Ganesh Kumar Veerasubramani,^a Myung-Soo Park,^a Goli Nagaraju,^b and Dong-Won Kim^{a*}

^aDepartment of Chemical Engineering, Hanyang University, Seoul 04763, Republic of Korea

^bDepartment of Chemical Engineering, Kyung Hee University, Gyeonggi-do 17104, Republic of Korea

Keywords: MoS₂ nanorods; enlarged spacing; anode material; sodium-ion battery; energy storage

*Corresponding author:

E-mail : dongwonkim@hanyang.ac.kr

Phone : +82 2 2220 2337

Fax : +82 2 2298 4101

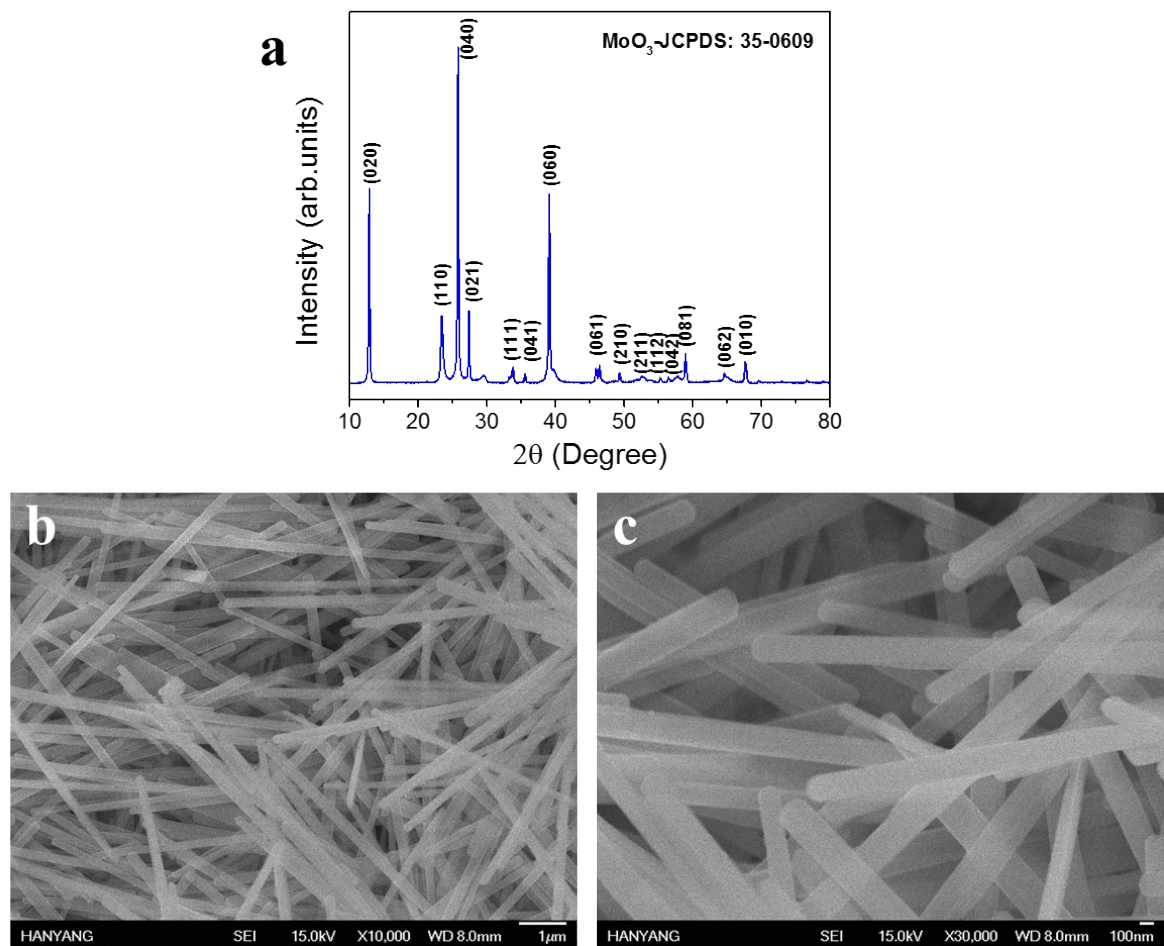


Fig. S1. (a) XRD pattern and (b, c) FE-SEM images at different magnification of MoO₃ NRs.

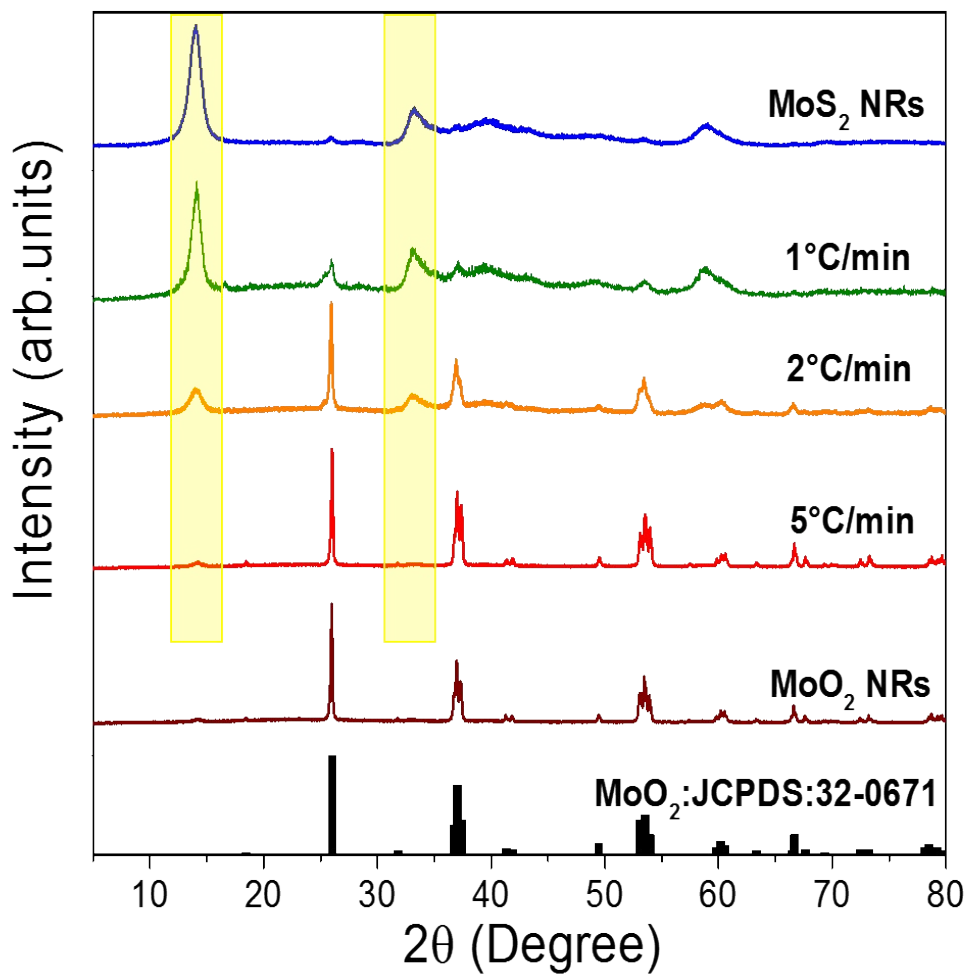


Fig. S2. XRD patterns of various raming rate tuned samples (pristine MoO₂ NRs, 5 °C min⁻¹, 2 °C min⁻¹, 1 °C min⁻¹, pristine MoS₂ NRs).

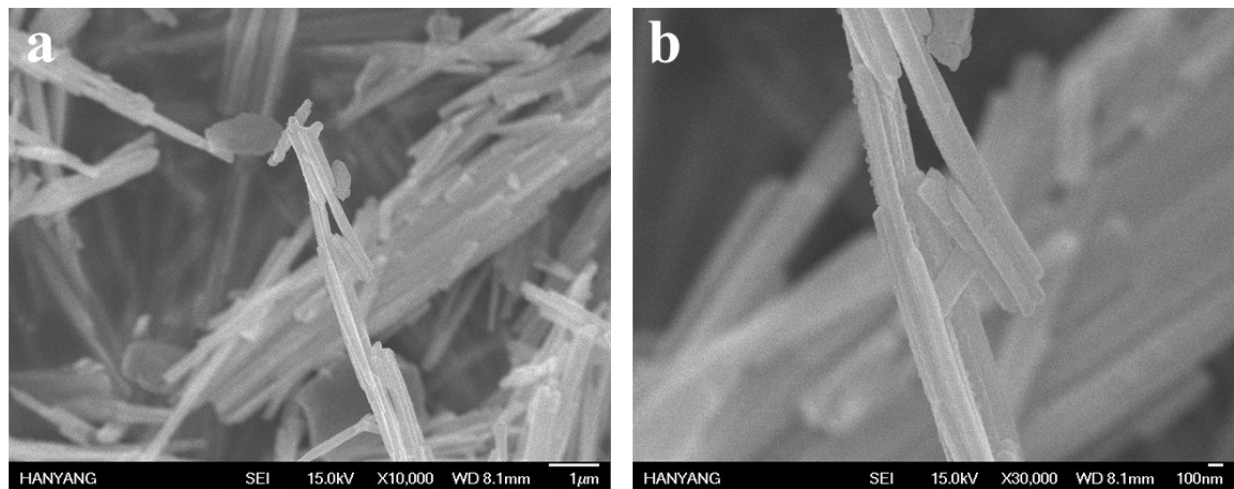


Fig. S3. (a, b) FE-SEM images of MoO_2 NRs at different magnification.

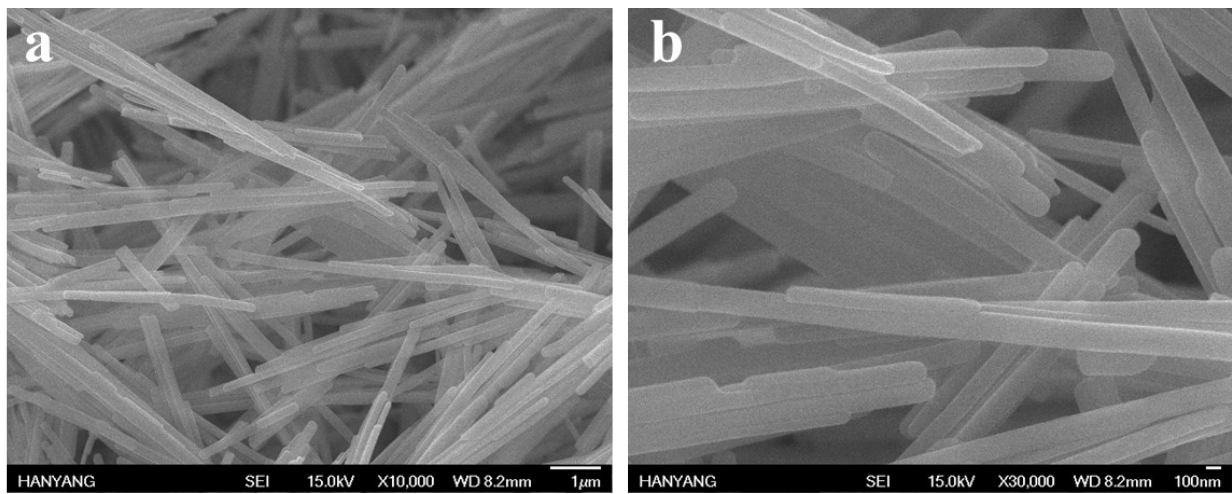


Fig. S4. (a, b) FE-SEM images at different magnification of MoS₂ NRs at ramping rate of 5 °C min⁻¹.

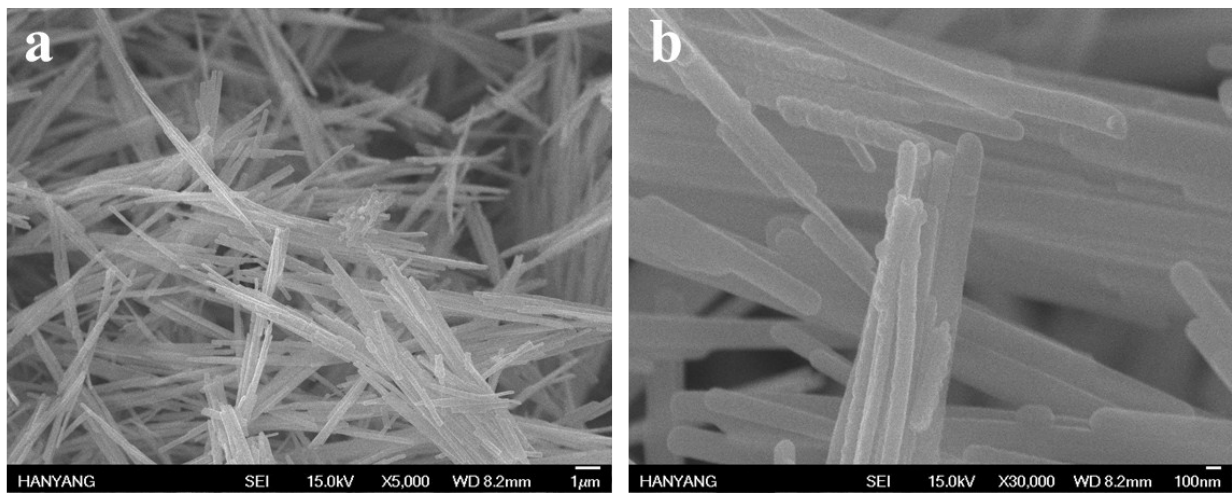


Fig. S5. (a, b) FE-SEM images at different magnification of MoS₂ NRs at ramping rate of 2 °C min⁻¹.

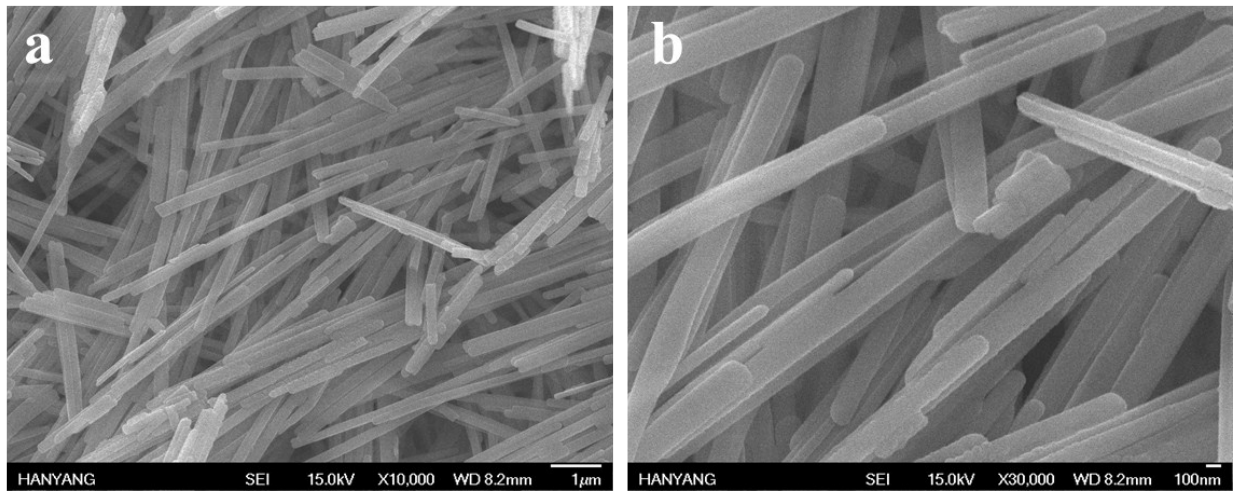


Fig. S6. (a, b) FE-SEM images at different magnification of MoS₂ NRs at ramping rate of 1 °C min⁻¹.

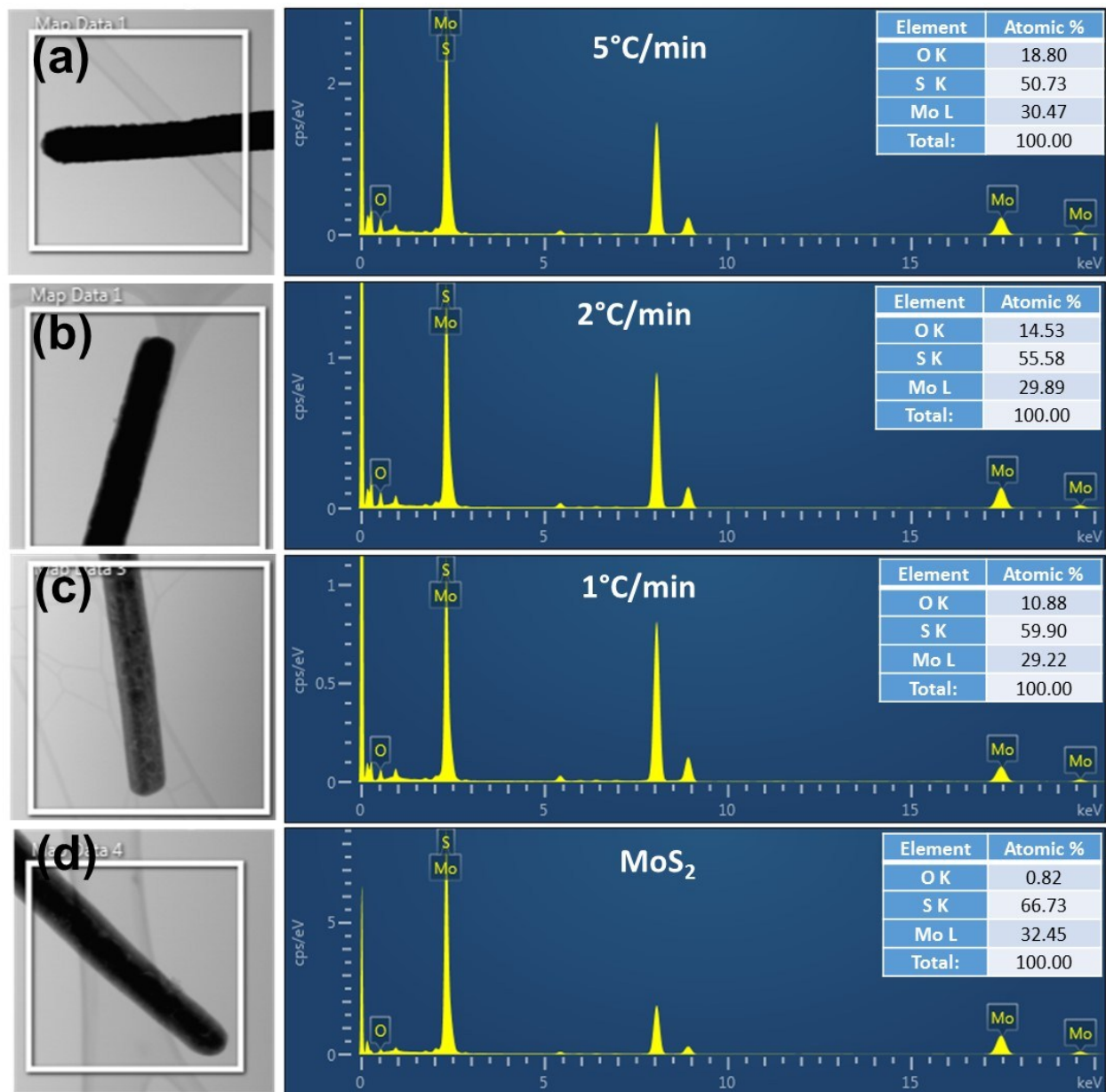


Fig. S7. EDS spectra of various sulfurized samples obtained at ramping rate of (a) $5\text{ }^{\circ}\text{C min}^{-1}$, (b) $2\text{ }^{\circ}\text{C min}^{-1}$, (c) $1\text{ }^{\circ}\text{C min}^{-1}$ and (d) full MoS_2 NRs.

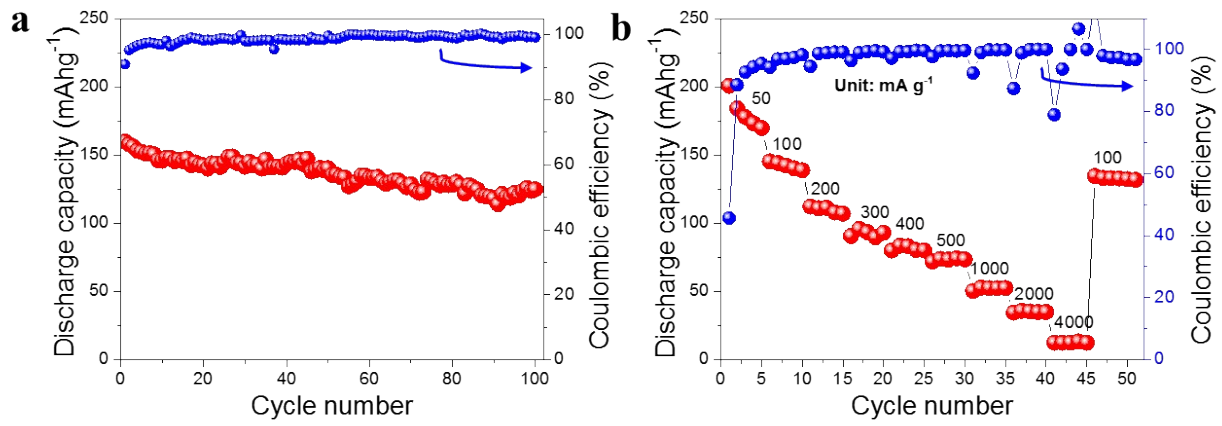


Fig. S8. (a) Cycling stability and (b) rate capability of MoO₃ NRs.

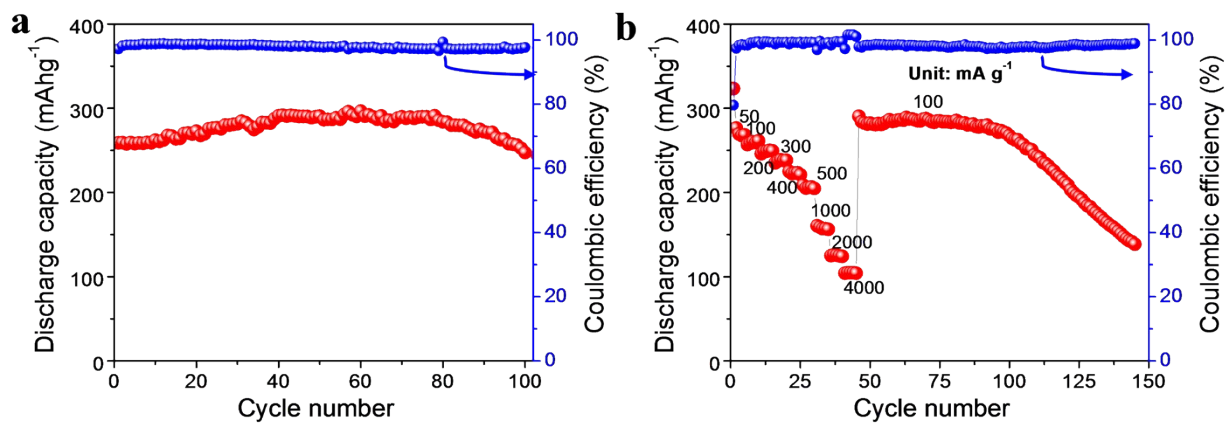


Fig. S9. (a) Cycling stability and (b) rate capability of MoS₂ NRs at ramping rate of 5 °C min⁻¹.

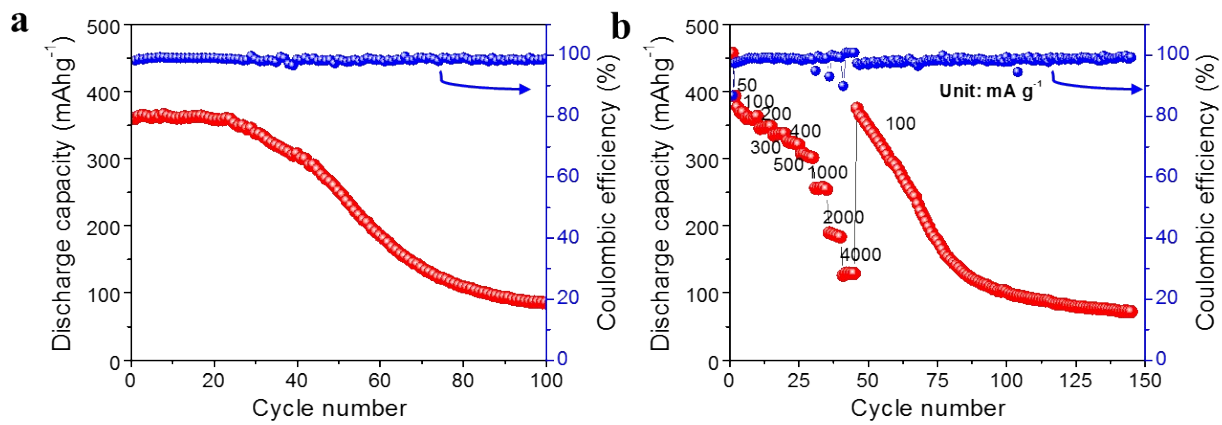


Fig. S10. (a) Cycling stability and (b) rate capability of MoS₂ NRs at ramping rate of 2 °C min⁻¹.

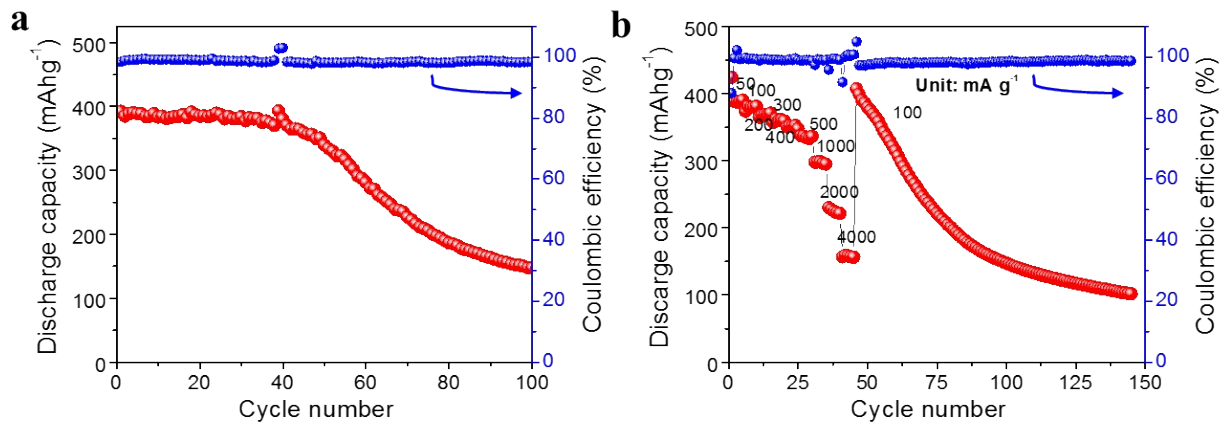


Fig. S11. (a) Cycling stability and (b) rate capability of MoS₂ NRs at ramping rate of 1 °C min⁻¹.

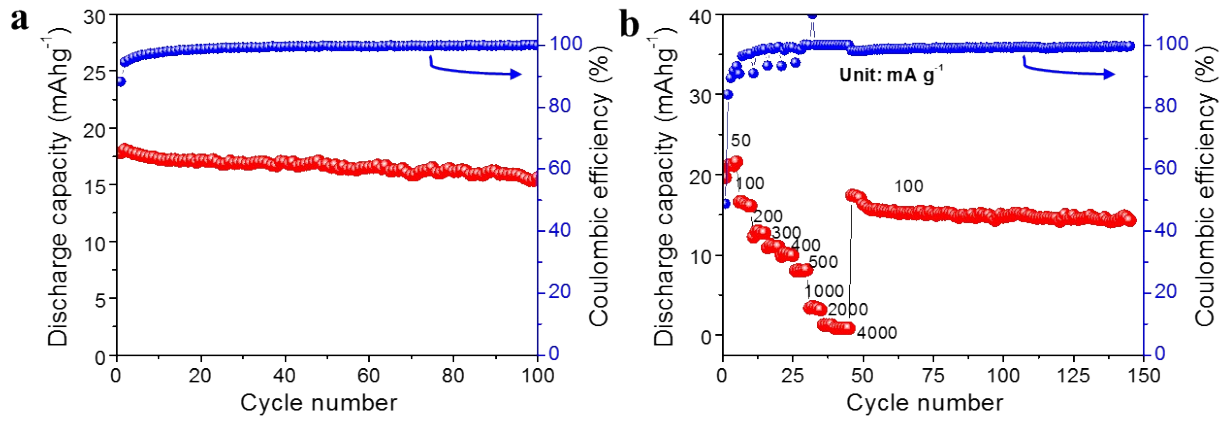


Fig. S12. (a) Cycling stability and (b) rate capability of MoO₂ NRs.

Table S1. Comparison of MoS₂@C@MoS₂ performance with other MoS₂ based anodes.

| Electrode Material | Initial Coulombic efficiency (%) | Cycling stability | Rate capability | References |
|--|----------------------------------|---|--|------------------|
| HMF-MoS ₂ | 60.2 | 384 mAh g ⁻¹ at 100 mA g ⁻¹ (After 100 cycles) | 226 mAh g ⁻¹ at 5 A g ⁻¹ | [1] |
| BD-MoS ₂ | <75 | 354 mAh g ⁻¹ at 500 mA g ⁻¹ (After 1000 cycles) | 262 mAh g ⁻¹ at 5 A g ⁻¹ | [2] |
| Expanded MoS ₂ @ Carbon fiber | 65.1 | 241 mAh g ⁻¹ at 1000 mA g ⁻¹ (After 700 cycles) | 109 mAh g ⁻¹ at 10 A g ⁻¹ | [3] |
| MoS ₂ @C paper | 79.5 | 268 mAh g ⁻¹ at 0.08 A g ⁻¹ (after 100 cycles) | 205 mAh g ⁻¹ at 1 A g ⁻¹ | [4] |
| 1T-MoS ₂ | 64 | 313 mAh g ⁻¹ at 50 mA g ⁻¹ (After 200 cycles) | 175 mAh g ⁻¹ at 2 A g ⁻¹ | [5] |
| MoS ₂ Nanoflowers | - | 350 mAh g ⁻¹ at 50 mA g ⁻¹ | 300 mAh g ⁻¹ at 1 A g ⁻¹ | [6] |
| MoS _{2-x} Se _x /GF | 55 | 208 mAh g ⁻¹ at 0.2 A g ⁻¹ (78.6% after 500 cycles) | ~115 mAh g ⁻¹ at 5 A g ⁻¹ | [7] |
| MoS ₂ /RGO Sponge | 67.4 | 372 mAh g ⁻¹ at 0.1 A g ⁻¹ (after 50 cycles) | 192 mAh g ⁻¹ at 1 A g ⁻¹ | [8] |
| MoS ₂ /RGO Sponge | 64 | 420 mAh g ⁻¹ at 0.1 A g ⁻¹ (after 160 cycles) | 284 mAh g ⁻¹ at 1 A g ⁻¹ | [9] |
| S/MoS ₂ | 78.6 | 413.2 mAh g ⁻¹ at 0.1 A g ⁻¹ (after 100 cycles) | 358.8 mAh g ⁻¹ at 0.5 A g ⁻¹ | [10] |
| MoS ₂ @C@MoS ₂ | 86.3 | 434 mAh g ⁻¹ at 100 mA g ⁻¹ (After 100 cycles) | 365 mAh g ⁻¹ at 4000 mA g ⁻¹ | <i>This work</i> |

Table S2. Comparison of MoS₂@C@MoS₂ performance with other metal sulfides/selenides based anodes.

| Electrode Material | Initial Coulombic efficiency (%) | Cycling stability | Rate capability | Reference |
|--------------------------------------|----------------------------------|---|---|------------------|
| NiS ₂ -rGO | 65 | 313 mAh g ⁻¹ at 100 mA g ⁻¹ (after 200 cycles) | 168 mAh g ⁻¹ at 2C rate | [11] |
| VS ₄ -rGO | 75.1 | 240.8 mAh g ⁻¹ at 100 mA g ⁻¹ (after 50 cycles) | 192.2 mAh g ⁻¹ at 800 mA g ⁻¹ | [12] |
| SnS-C | 79 | 260 mAh g ⁻¹ at 100 mA g ⁻¹ (after 300 cycles) | 145 mAh g ⁻¹ at 1000 mA g ⁻¹ | [13] |
| SnS-MWCNT | 73.3 | 391 mAh g ⁻¹ at 100 mA g ⁻¹ (after 50 cycles) | 410 mAh g ⁻¹ at 500 mA g ⁻¹ | [14] |
| CoMoS ₃ | 77.7 | 411 mAh g ⁻¹ at 2 A g ⁻¹ (after 300 cycles) | 349 mAh g ⁻¹ at 10 A g ⁻¹ | [15] |
| CoSe ₂ @N-PGC/CNTs | 75.6 | 424 mAh g ⁻¹ at 0.1 A g ⁻¹ (after 100 cycles) | 368 mAh g ⁻¹ at 5 A g ⁻¹ | [16] |
| Fe ₇ Se ₈ @NC | 78.7 | 367 mAh g ⁻¹ at 0.5 A g ⁻¹ (after 100 cycles) | 251 mAh g ⁻¹ at 2 A g ⁻¹ | [17] |
| FeS/N-C | 51.5 | 511 mAh g ⁻¹ at 0.2 A g ⁻¹ (after 100 cycles) | 260 mAh g ⁻¹ at 4 A g ⁻¹ | [18] |
| CoS ₂ @N,S-doped carbon | 70 | 510 mAh g ⁻¹ at 0.1 A g ⁻¹ (after 100 cycles) | 288 mAh g ⁻¹ at 2 A g ⁻¹ | [19] |
| MoSe ₂ /N,P-doped rGO | 69.6 | 337 mAh g ⁻¹ at 0.1 A g ⁻¹ (after 100 cycles) | 244.4 mAh g ⁻¹ at 1 A g ⁻¹ | [20] |
| MoS ₂ @C@MoS ₂ | 86.3 | 434 mAh g ⁻¹ at 100 mA g ⁻¹ (after 100 cycles) | 365 mAh g ⁻¹ at 4000 mA g ⁻¹ | <i>This work</i> |

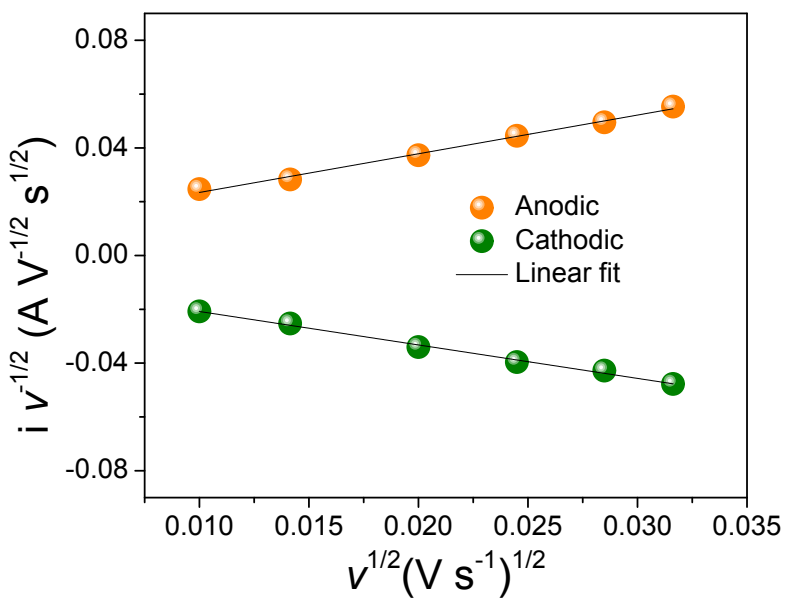


Fig. S13. Linear fit curve for peak current vs square root of scan rates for MoS₂@C@MoS₂ electrode.

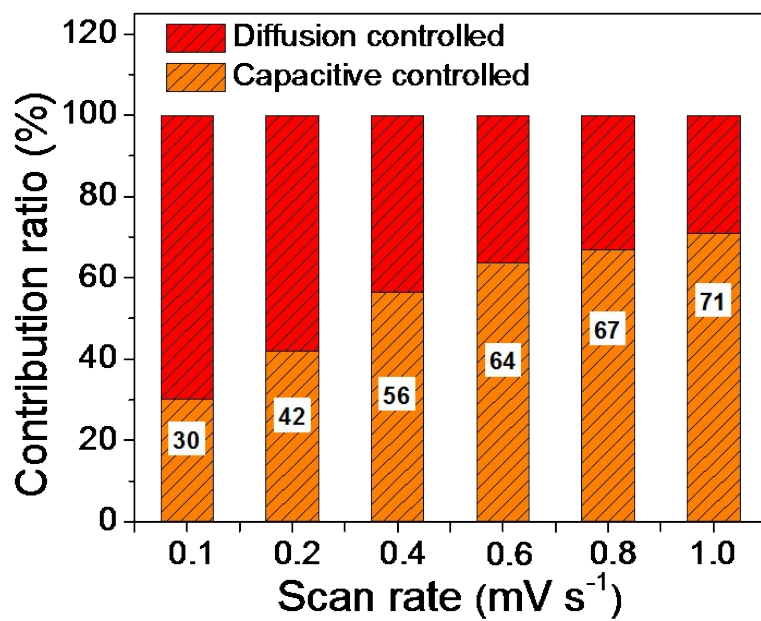


Fig. S14. Contribution of capacitive and diffusion controlled reaction for pristine MoS_2 NRs.

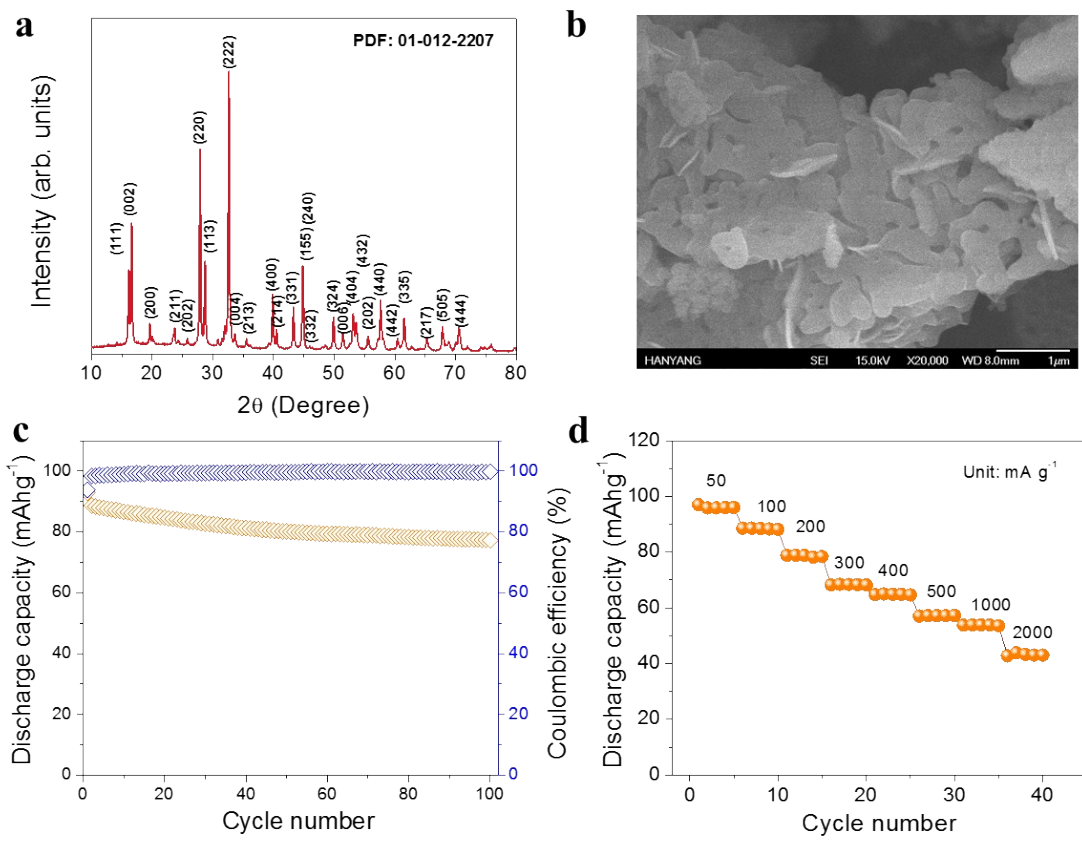


Fig. S15. (a) XRD pattern, (b) FE-SEM image, (c) cycling stability and (d) rate capability of NVPF cathode.

References

- [1] Y. Li, R. Zhang, W. Zhou, X. Wu, H. Zhang and J. Zhang, *ACS Nano* 2019, **15**, 5533.
- [2] K. Yao, J. Huang, M. Ma, L. Fu, X. Shen, J. Li and M. Fu, *Small* 2019, **15**, 1805405
- [3] C. Zhao, C. Yu, M. Zhang, Q. Sun, S. Li, M.N. Banis, X. Han, Q. Dong, J. Yang, G. Wang, X. Sun and J. Qiu, *Nano Energy* 2017, **41**, 66.
- [4] X. Xie, T. Makaryan, M. Zhao, K.L. Van Aken, Y. Gogotsi and G. Wang, *Adv Energy Mater.* 2016, **6**, 1502161.
- [5] X. Geng, Y. Jiao, Y. Han, A. Mukhopadhyay, L. Yang and H. Zhu, *Adv. Funct. Mater.* 2017, **27**, 1702998.
- [6] Z. He, L. Wang, K. Zhang, J. Wang, F. Cheng, Z. Tao and J. Chen, *Angew. Chem.* 2014, **126**, 130088.
- [7] G. Jia, D. Chao, N.H. Tiep, Z. Zhang and H.J. Fan, *Energy Storage Materials* 2018, **14**, 136.
- [8] J. Li, W. Qin, J. Xie, R. Lin, Z. Wang, L. Pan and W. Mai, *Chem. Eng. J.* 2018, **332**, 260.
- [9] Z. Che, Y. Li, K. Chen and M. Wei, *J. Power Sources* 2016, **331**, 50.
- [10] Z. Xu, K. Yao, Z. Li, L. Fu, H. Fu, J. Li, L. Cao and J. Huang, *J. Mater. Chem. A* 2018, **6**, 10535
- [11] T. Wang, P. Hu, C. Zhang, H. Du, Z. Zhang, X. Wang, S. Chen, J. Xiong and G. Cui, *ACS Appl. Mater. Interfaces* 2016, **8**, 7811.
- [12] R. Sun, Q. Wei, Q. Li, W. Luo, Q. An, J. Sheng, D. Wang, W. Chen and L. Mai, *ACS Appl. Mater. Interfaces* 2015, **7**, 20902.
- [13] C. Zhu, P. Kopold, W. Li, P.A. Aken, J. Maier and Y. Yu, *Adv. Sci.* 2015, **2**, 1500200.
- [14] W. Wang, L. Shi, D. Lan and Q. Li, *J. Power Sources* 2018, **377**, 1.
- [15] S.H. Yang, S.-K. Park, J.K. Kim and Y.C. Kang, *J. Mater. Chem. A* 2019, **7**, 13751.

- [16] S.K. Park, J.K. Kim and Y.C. Kang, *Chem. Eng. J.* 2017, **328**, 546.
- [17] M. Wan, R. Zeng, K. Chen, G. Liu, W. Chen, L. Wang, N. Zhang, L. Xue, W. Zhang and Y. Huang, *Energy Storage Materials* 2018, **10**, 114.
- [18] Y. Liu, W. Zhong, C. Yang, Q. Pan, Y. Li, G. Wang, F. Zheng, X. Xiong, M. Liu and Q. Zhang, *J. Mater. Chem. A* 2018, **6**, 24702.
- [19] F. Han, T. Lv, B. Sun, W. Tang, C. Zhang and X. Li, *RSC Adv.* 2017, **7**, 30699.
- [20] A. Roy, A. Ghosh, A. Kumar and S. Mitra., *Inorg. Chem. Front.* 2018, **5**, 2189.